International Journal of Nanomedicine

Dovepress
open access to scientific and medical research

Open Access Full Text Article

ORIGINAL RESEARCH

Silver nanoparticles/chitosan oligosaccharide/poly(vinyl alcohol) nanofiber promotes wound healing by activating TGFβ1/Smad signaling pathway

This article was published in the following Dove Press journal:
International Journal of Nanomedicine
21 January 2016
Number of times this article has been viewed

Chen-wen Li[1,*]
Qing Wang[2,*]
Jing Li[3]
Min Hu[1]
San-jun Shi[1]
Zi-wei Li[1]
Guo-lin Wu[1]
Huan-huan Cui[1]
Yuan-yuan Li[1]
Qian Zhang[1]
Xiu-heng Yu[2]
Lai-chun Lu[1]

[1]Department of Pharmacy, Institute of Surgery Research, Daping Hospital, Third Military Medical University, [2]College of Pharmacy, Chongqing Medical University, Chongqing, [3]Department of Pharmacy, the Affiliated Hospital of Qingdao University, Qingdao, People's Republic of China

*These authors contributed equally to this work

Abstract: Wound healing occupies a remarkable place in everyday pathology and remains a challenging clinical problem. In our previous study, we prepared a silver nanoparticle/chitosan oligosaccharide/poly(vinyl alcohol) (PVA/COS-AgNPs) nanofiber via electrospinning and revealed that it could promote wound healing; however, the healing mechanism remained unknown. Therefore, we aimed to clarify the mechanism underlying the accelerated healing effect of the PVA/COS-AgNPs nanofiber. The TGFβ1/Smad signaling pathway is actively involved in wound healing. Considering the key role of this signaling pathway in wound healing, our preliminary study showed that the TGFβ1 level was significantly increased during the early stage of wound healing. Thus, in this study, hematoxylin–eosin, Masson's trichrome, immunofluorescent staining, hydroxyproline content, quantitative real-time polymerase chain reaction, and Western blot analyses were used to analyze the wound healing in a rat model treated with gauze, the PVA/COS-AgNPs nanofiber, and the nanofiber plus SB431542 (an inhibitor of TGFβ1 receptor kinase). The results showed that the PVA/COS-AgNPs nanofiber promoted wound healing and upregulated the expression levels of cytokines associated with the TGFβ1/Smad signaling pathway such as TGFβ1, TGFβRI, TGFβRII, collagen I, collagen III, pSmad2, and pSmad3. Inhibiting this pathway with SB431542 resulted in prevention of the PVA/COS-AgNPs nanofiber-associated salutary effects on the early stage of wound healing and relative cytokines expression. In conclusion, the wound healing effect of the PVA/COS-AgNPs nanofiber involves activation of the TGFβ1/Smad signaling pathway.

Keywords: wound healing, electrospinning, nanofiber, silver nanoparticles, TGFβ1, Smad proteins

Introduction

The skin is the largest organ and functions as a barrier between the environment and internal organs.[1] The skin is also easily injured by many types of attacks; thus, skin damage is an extremely common disease that is observed clinically.[2] Although the skin can repair itself after being damaged,[3] many problems still remain, such as severe infection and even death. Wound repair is an extremely complex process that requires the coordination of a series of cellular responses.[4] Therefore, many studies have focused on the principles and mechanisms of wound healing acceleration to develop new drugs that promote wound healing.

Recently, researchers have begun to pay close attention to an electrospun nanofiber that promotes wound healing. Nanofibers produced via electrospinning exhibit high specific surface areas, high levels of porosity, and gas permeation. These properties are

Correspondence: Lai-chun Lu
Department of Pharmacy, Institute of Surgery Research, Daping Hospital, Third Military Medical University, 10 Changjiangzhilu, Chongqing 400042, People's Republic of China
Tel +86 23 6875 7092
Fax +86 23 6889 8867
Email lulab2010@126.com

favorable for hemostasis, exudate adsorption, and prevention of bacterial penetration, and the nanoscale fiber can induce cellular adherence, proliferation, and skin regeneration, thus providing favorable conditions for wound healing.[5,6]

Chitosan oligosaccharide (COS) is a mixture of oligomers composed of β-1,4-linked D-glucosamine residues, and it is the only alkaline oligosaccharide in nature.[7] COS has excellent biocompatibility and biodegradability, and its hemostatic action, antibacterial effect, anti-inflammatory effect, and stimulation of cellular activities have resulted in its wide use in pharmaceutical, food, biotechnology, and agricultural applications.[8–10] Poly(vinyl alcohol) (PVA) is a hydrophilic, biocompatible polymer that exhibits good mechanical properties and is biodegradable and safe. In our previous studies,[11] we synthesized COS-Ag nanoparticles via a reduction reaction and prepared PVA/COS-AgNPs nanofiber via electrospinning. Silver nanoparticles exhibit antimicrobial properties that are more effective than other salts due to their large surface area, which results in better contact with microorganisms. Our previous results showed that the PVA/COS-AgNPs nanofiber significantly inhibited bacteria growth. Additionally, the hemostatic and anti-inflammatory actions, stimulation of proper collagen deposition by COS, hygroscopicity, wound protection of PVA, and the high permeability and high swelling rate of the nanofiber together promote wound healing at an early stage. Moreover, cells interact with the extracellular matrix (ECM) on the nanoscale level, and our COS-AgNPs could fully interact with cells and the ECM. They could create good conditions for the exchange of cell information and substance.[12] However, in the current literature, the effect of wound healing acceleration by electrospun nanofiber has only been examined at the pharmacodynamics stage. Therefore, the mechanisms of nanofiber-promoted wound healing remain unknown.

Many growth factors are involved during various stages of wound healing. TGFβ is known for exerting a powerful effect to control a variety of cellular functions, and it can induce many different outcomes depending on the cellular context and cell type.[13] Four isoforms of TGFβ exist: TGFβ1, TGFβ2, TGFβ3, and TGFβ4.[14] Notably, TGFβ1 plays an important role in almost all stages of wound healing and scar formation.[15,16] Furthermore, many studies have shown that the TGFβ1/Smad signaling pathway is closely connected to wound healing.[17] Smad family proteins, such as Smad2, Smad3, and Smad4, are mediators of the TGFβ1 signaling from the cytoplasm to the nucleus, whereas Smad7 inhibits this signaling pathway.[18,19]

On the basis of our previous studies[11] and the work of other groups,[20–22] in this study, we used a rat skin wound model and a potent inhibitor of the TGFβ1 receptor, SB431542, which can efficiently inhibit the activation of the TGFβ1/Smad signaling pathway.[23] PVA/COS-AgNPs nanofiber was applied to examine the influence of the signaling molecules involved in the TGFβ1/Smad signaling pathway using a number of detection methods, such as quantitative real-time polymerase chain reaction (qRT-PCR) and Western blot (WB). Collagen is a major component of the ECM that contributes to skin regeneration, and collagen formation can be measured to evaluate the degree of wound healing. The conventional method of total collagen content detection is based on hydroxyproline (Hyp), a basic constituent of collagen and an indicator that reflects the total collagen amount.[24,25] Thus, we used several assays, such as Hyp analysis and immunofluorescent staining, to investigate collagen synthesis with the nanofiber treatment. This study was designed to verify the effect of a PVA/COS-AgNPs nanofiber treatment on the TGFβ1/Smad signaling pathway, to explore the molecular mechanism by which this nanofiber treatment promotes wound healing, and to lay a foundation to investigate this new type of medicine for wound healing.

Materials and methods

Preparation of PVA/COS-AgNPs nanofiber

First, we synthesized COS-AgNPs by stirring 35 mL of a 0.1 M $AgNO_3$ solution containing 1 g of COS for 5 hours at 50°C, and then, the solution was cooled to room temperature. A suitable amount of acetone was added to the solution to precipitate the product; then, the solvent was vaporized to obtain dry COS-AgNPs. Next, the COS-AgNPs (5 wt% to polymer) were added to an 11% PVA solution and stirred for 12 hours to obtain a uniform mixture. Then, a high-voltage power source (DW-P303-1ACD8; Tianjin Dongwen High Voltage Co., Guangzhou, People's Republic of China) was adjusted to 15 kV and connected to a syringe with a needle containing the PVA/COS-AgNPs solution. The flow rate (0.5 mL/h) was controlled by a syringe pump (TJ-3A; Baoding Longer Precision Pump Co., Ltd, Hebei, People's Republic of China). The PVA/COS-AgNPs nanofiber was collected on an electrically grounded metal plate.[11]

Establishment of a skin incision wound model

Male Sprague–Dawley rats (200–250 g) were used to establish a skin incision wound model. Animal use was approved by the ethical committee of the Experimental Animal Centre of the Third Military Medical University, and the experiments

were performed according to the prescribed guidelines. Chloral hydrate (10% w/v) at a dosage of 350 mg/kg of body weight was injected into the abdominal cavities of the rats. After anesthetization, the hair on the dorsal side of the rats was shaved. Four positions on the dorsal side of rats were marked with a pencil to form the 1 cm length sides of a square to delineate the wound margins. Then, a 75% ethanol solution was applied for sterilization. The intended surgical area of the skin was shaved with disinfected surgical scissors to create four whole-layer skin incision wounds, deep into the dermis without damaging the subdermal vasculature.[26]

Animal grouping and treatment

The rats were segregated into three groups. Group A was topically treated with gauze as a blank group. Group B received an application of 5% PVA/COS-AgNPs nanofiber. Group C received an application of 5% PVA/COS-AgNPs nanofiber plus the TGFβ1 receptor inhibitor (SB431542; Selleck Chemicals, Houston, TX, USA). The stock SB431542 powder was dissolved in DMSO (10 mg/mL). A 10 µL stock solution was diluted 100 times with normal saline to a final concentration of 100 µg/mL before each use. A dosage of 40 µg/100 g SB431542 was injected hypodermically next to each wound every day. The gauze group and the PVA/COS-AgNPs nanofiber group were injected with the same solvent as used for the PVA/COS-AgNPs nanofiber plus SB431542 group. Six rats that did not undergo surgical operation were used as a normal control group. Bandages were replaced every 24 hours. The rats were studied for 18 days after the surgery. The wound diameters were measured on days 1, 3, 5, 7, 9, 12, 15, and 18 post-wounding. The calculated average diameter of the remaining healing area was used to determine the healing percentage. Six rats from each group were sacrificed on days 3, 5, 7, 9, 12, 15, and 18 under anesthesia. The wounded skin tissues, including a margin of approximately 3 mm of unwounded skin, were collected using surgical scissors to ensure complete removal. After the tissues were washed with physiological saline, they were immediately flash frozen in liquid nitrogen and divided into two portions: one portion was used for sectioning, and the other portion was stored at –80°C for subsequent molecular evaluation.

Histopathological examination

Full-thickness skin biopsies were fixed in 10% buffered formalin and embedded in paraffin. Sections (4 µm through the center of the wound) were stained with hematoxylin–eosin (HE) and Masson's trichrome. Epithelialization, inflammatory cell infiltration, fibroblast proliferation, neovascularization, and collagen deposition were observed under a light microscope (Olympus BX51; Olympus, Tokyo, Japan; magnification: ×100).

Immunofluorescent staining

Transverse cryosections were embedded in optimal cutting temperature compound, frozen in liquid nitrogen, and stored at –80°C. A mixture of rabbit anti-collagen Type I (AB755P; Millipore, Billerica, MA, USA; 1:100) and mouse anti-collagen Type III (ab6310; Abcam, Cambridge, UK; 1:300) antibodies was used to detect collagen fibers. After the samples were blocked in 5% skim milk/tris-buffered saline with tween 20, they were incubated with primary antibodies and then with fluorescent probe-conjugated secondary antibodies: goat anti-rabbit IgG (ab150077; Abcam, 1:1,000), goat anti-mouse IgG (ab150119; Abcam, 1:1,000). The nuclei were stained with DAPI (4′,6-diamidino-2-phenylindole; Boster, Wuhan, People's Republic of China). The quantities and distributions of collagen I and collagen III were determined by imaging with a confocal laser scanning microscope (Leica Microsystems, Wetzlar, Germany; magnification: ×800).

Hydroxyproline content measurement

Hyp is extremely stable in collagen; thus, its content can indirectly reflect the total collagen content.[27] To estimate the Hyp content, a kit (Nanjing Jiancheng Bioengineering Institute, Nanjing, People's Republic of China) was used in this study, and the manufacturer's protocol was followed. The color intensity was measured at 550 nm against a blank. The Hyp content in the tissue was calculated according to the manufacturer's protocol.

RNA extraction, reverse transcription, and qRT-PCR

After treatment, the total RNA of the tissue samples was isolated using RNAiso Plus (TaKaRa Bio Inc., Tokyo, Japan), purified, and precipitated using chloroform and isopropanol; then, the RNA was dissolved in 50 µL RNase-free deionized H_2O and spectrophotometrically quantified at 260/280/320 nm. Briefly, total RNA extracted from the tissue samples was reverse transcribed into complementary DNA (cDNA) using a PrimeScript RT Reagent Kit with gDNA Eraser (TaKaRa Bio Inc.). The final cDNA product was stored at –20°C for subsequent cDNA amplification by qRT-PCR. cDNA was amplified using SYBR® Premix Ex TaqTM II (TaKaRa, Japan). Each amplification was performed using the following conditions: 30 seconds at 95°C, followed by 40 cycles of 5 seconds at 95°C, 20 seconds at

Table 1 Primers used for qRT-PCR

Template	Forward primer (5′–3′)	Reverse primer (5′–3′)
TGFβ1	ATGACATGAACCGACCCTTC	ACTTCCAACCCAGGTCCTTC
TGFβRI	ACCTTCTGATCCATCCGTT	CGCAAAGCTGTCAGCCTAG
TGFβRII	GTGAGAAGCCGCAGGAAGTC	CCGTGGTAGGTGAACTTGGG
Smad2	CTGGCTCAGTCTGTCAACCA	CTGCCTCCGATATTCTGCTC
Smad3	CCAGTGCTACCTCCAGTGTT	CTGGTGGTCGCTAGTTTCTC
Smad7	GGAGTCCTTTCCTCTCTC	GGCTCAATGAGCATGCTCAC
Collagen I	GAGCGGAGAGTACTGGATCG	TACTCGAACGGGAATCCATC
Collagen III	ACCTCCTGGTGCTATTGGTC	TCTCTCCATTGCGTCCATC
Fibronectin	TGACTCGCTTTGACTTCACCAC	TCTCCTTCCTCGCTCAGTTCGT
VEGF	AGGCCAGCACATAGGAGAGA	TTTCTTGCGCTTTCGTTTTT
β-Actin	CCTTCCTGGGTATGGAATCCT	GGAGCAATGATCTTGATCTT

Abbreviations: qRT-PCR, quantitative real-time polymerase chain reaction; TGFβ1, transforming growth factor-beta1; TGFβRI, transforming growth factor beta receptor I; TGFβRII, transforming growth factor beta receptor II; VEGF, vascular endothelial growth factor.

60°C, and 15 seconds at 72°C. mRNA (messenger RNA) was amplified using specific primers at a final concentration of 2.5 μM. The primers (BGI Tech, Shenzhen, People's Republic of China) for the qRT-PCR analysis are listed in Table 1. The relative quantitation values for gene expression were calculated from the CT values according to the manufacturer's protocol (LightCycler 480 software; Roche, Basel, Switzerland). The relative expression of target genes was normalized to that of β-actin. ΔCT values for triplicate wells of the calibrator (normal skin) for each sample were averaged, and the relative expression was calculated as $2^{-\Delta\Delta CT}$.

Protein extraction and WB analysis

Total protein was extracted using lysis buffer containing 1 mM phenylmethanesulfonyl fluoride (Beyotime, Haimen, People's Republic of China), quantified using a BCA Protein Assay Kit (Beyotime), and normalized to a standard concentration using extraction buffer. Then, the proteins were denatured for 5 minutes at 100°C, and a 20 μL protein sample from each group was separated by 10% or 12% sodium dodecyl sulfate–polyacrylamide gel electrophoresis and transferred to polyvinylidene fluoride membranes (Millipore). The membranes were blocked with 5% BSA (albumin from bovine serum; Sinopharm, Beijing, People's Republic of China) at 37°C for 1 hour and incubated overnight with the following primary antibodies at 4°C: anti-TGFβ1 (ab92486; Abcam, 1:500), anti-phospho-Smad2 (#3108; Cell Signaling Technology, Danvers, MA, USA; 1:500), anti-Smad2 (#5339; Cell Signaling Technology, 1:1,000), anti-phospho-Smad3 (#9520; Cell Signaling Technology, 1:500), anti-Smad3 (#9513; Cell Signaling Technology; 1:500), anti-collagen III (ab6310; Abcam, 1:1,000), anti-collagen I (BA0325; Boster, 1:2,000), anti-phospho-Smad1/5/8 (#9511S; Cell Signaling Technology, 1:500), and anti-β-actin (#4967; Cell Signaling Technology, 1:1,000). Then, the membranes were incubated with horseradish peroxidase (HRP)-conjugated secondary antibodies (ZSGB-BIO, Beijing, People's Republic of China; 1:5,000), and the specific proteins were visualized with Immobilon Western Chemiluminescent HRP Substrate (Millipore).

Statistics

The data are expressed as mean ± standard deviation. SPSS 18.0 (SPSS Inc., Chicago, IL, USA) statistical software was used to perform statistical analysis. A two-tailed unpaired Student's *t*-test for two-group comparison was used. $P<0.05$ indicates a statistically significant difference.

Results

PVA/COS-AgNPs nanofiber treatment decreases the wound area of wounded rat skin and achieves better cosmesis

Full-thickness incisional wounds at 0, 3, 5, 7, 12, and 18 days after the surgery are shown in Figure 1A. Wound closure was observed in all of the treatment groups within 18 days. The wound contraction of the PVA/COS-AgNPs nanofiber group was significantly faster than that of the nanofiber plus SB431542 group. Meanwhile, the nanofiber plus SB431542 group displayed ulcerated surfaces at days 3 and 5. The healing level of the gauze group was in between those of the other two groups. The change in the wound closure size was displayed as a percentage of the wound area at different healing times. Each wound area measurement was compared with the wound area on day 0 (100%; Figure 1B).

To histologically assess the wound healing, skin samples from each group at every time point were examined by HE staining. Figure 2 shows the wound healing histology for each

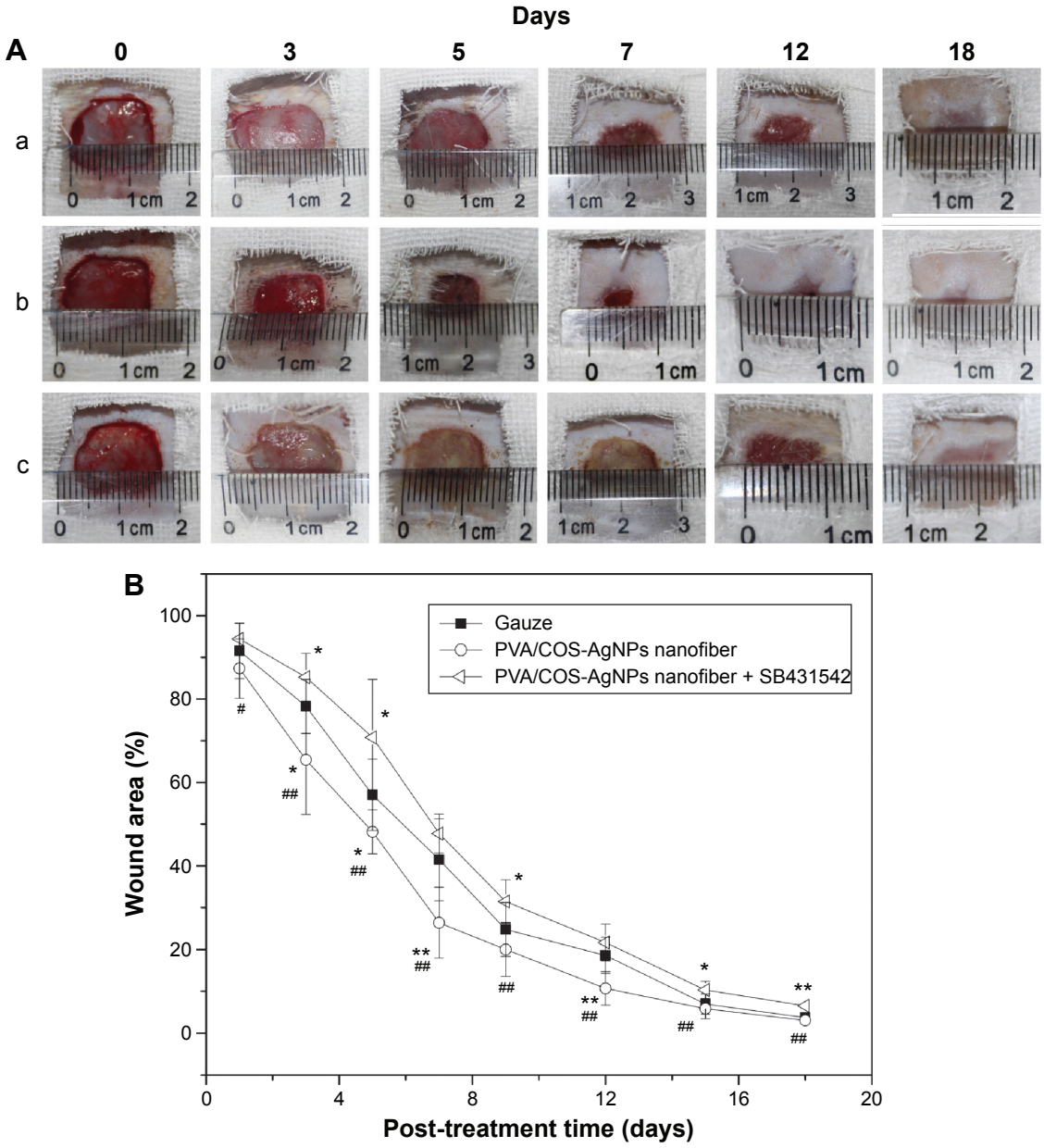

Figure 1 PVA/COS-AgNPs nanofiber treatment decreases wound area of wounded rat skin and achieves better cosmesis.
Notes: (**A**) Full-thickness incisional wounds of group (a) gauze, (b) PVA/COS-AgNPs nanofiber, (c) PVA/COS-AgNPs nanofiber plus SB431542 at 0, 3, 5, 7, 12, and 18 days after surgery. (**B**) The change in wound closure size displayed as a percentage of wound area at different healing times. Each wound area measurement was compared with the wound area on day 0. Values are mean ± standard deviation. $^{*}P<0.05$ and $^{**}P<0.01$ vs gauze group, $^{\#}P<0.05$ and $^{\#\#}P<0.01$ vs PVA/COS-AgNPs nanofiber plus SB431542 group.
Abbreviations: PVA, poly(vinyl alcohol); COS, chitosan oligosaccharide; AgNPs, silver nanoparticles.

group at days 3, 7, 12, and 18 after wounding, with stained collagen fibers in pale pink, the cytoplasm in purple, the nuclei in blue, and the red blood cells in cherry red. At the early stage of the healing processes (days 0–7), the wounds in the three groups displayed evident inflammatory cell infiltration, granulation tissue formation, and epidermal proliferation. However, the inflammatory cells and granulation tissue in the PVA/COS-AgNPs nanofiber group disappeared quickly, and new blood vessels and hair follicles began to grow in this group before the other groups. At the late stage of the healing process (days 9–18), the PVA/COS-AgNPs nanofiber group showed the greatest resemblance to normal skin, with less hypertrophic scarring, a thin epidermis, and nearly normal hair growth on the wound surface (Figure S1). The healing condition of the gauze group was similar to that of the PVA/COS-AgNPs nanofiber group at day 18, but the gauze group showed slower healing progression. The worst cosmetic appearance was observed in the nanofiber plus SB431542 group; new blood vessels and hair follicles had grown very slowly (Figure S1).

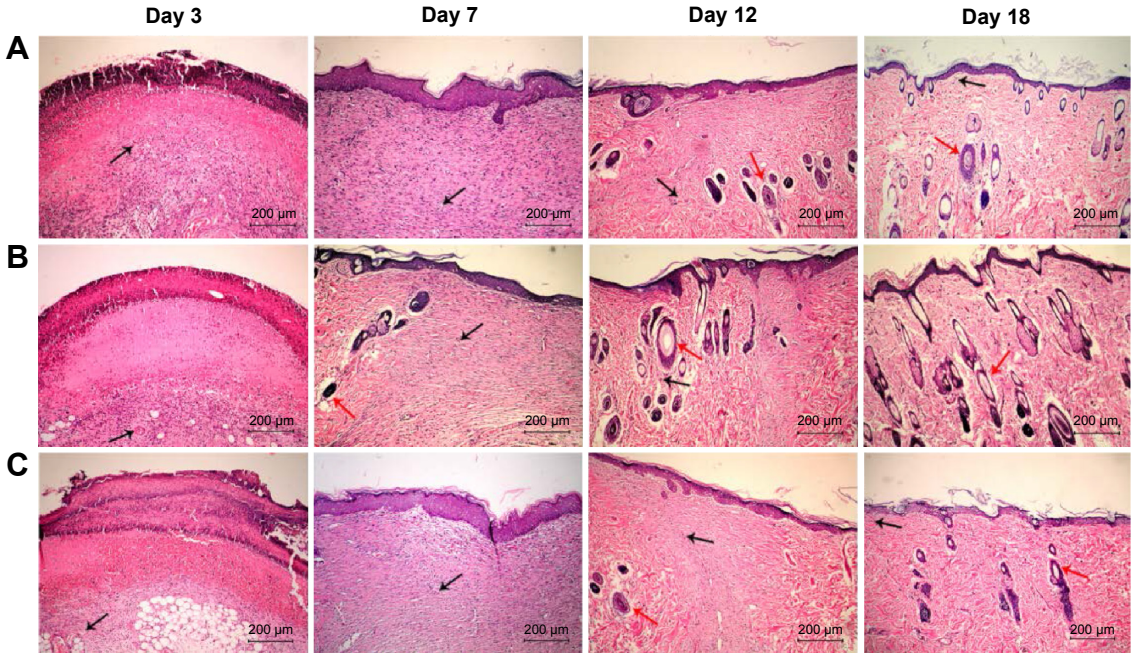

Figure 2 Wound healing histology for each group at days 3, 7, 12, and 18 after surgery.
Notes: HE staining shows collagen fibers stained pale pink, cytoplasm stained purple, nuclei stained blue, and red blood cells stained cherry red. **A**, **B**, and **C** show gauze group, PVA/COS-AgNPs nanofiber group, PVA/COS-AgNPs nanofiber plus SB431542 group, respectively. The black and red arrows indicate blood vessels and hair follicles, respectively.
Abbreviation: HE, hematoxylin–eosin.

PVA/COS-AgNPs nanofiber treatment promotes collagen fibers regeneration in rat skin

Wound healing is largely dependent on collagen synthesis. Therefore, to further investigate the effect of PVA/COS-AgNPs nanofiber treatment on wound healing, biopsies of rat skin tissues were stained with Masson's trichrome staining (Figure 3). Collagen was stained blue-green, whereas the cytoplasm, red blood cells, and muscle were stained red; the staining was used to assess the advancement of collagen

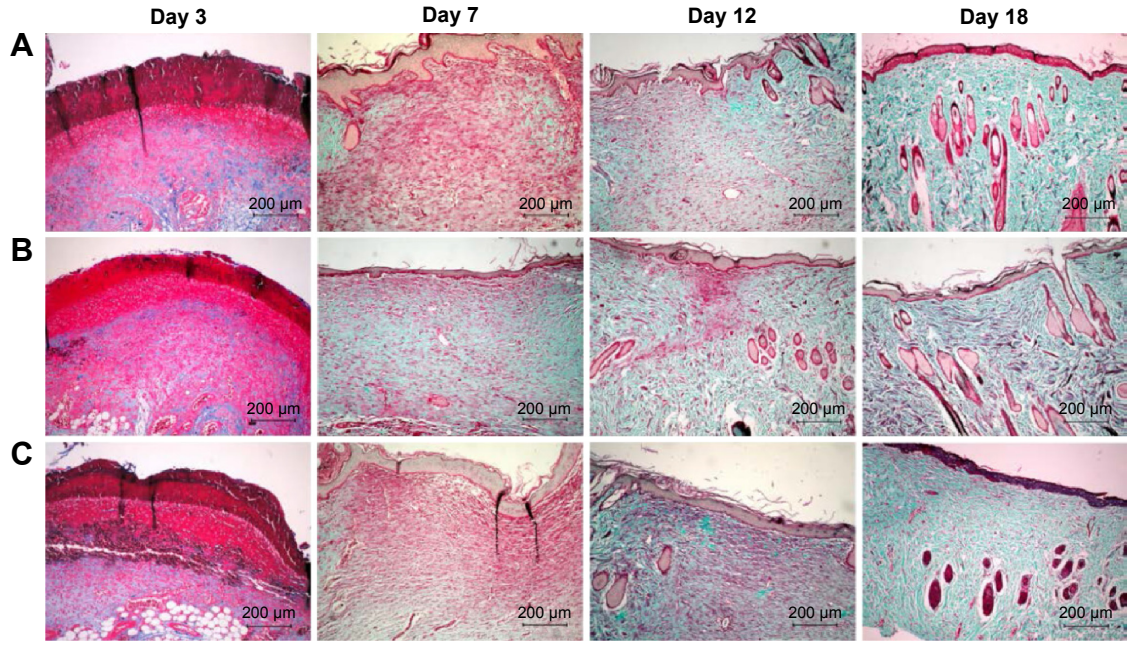

Figure 3 Masson's trichome staining of biopsies of rat skin tissue.
Notes: Collagen is stained blue-green, while cytoplasm, red blood cells, and nuclei are stained red. Masson-trichrome staining of collagen at day 3, 7, 12, 18 post-wounding: (**A**) gauze, (**B**) PVA/COS-AgNPs nanofiber, (**C**) PVA/COS-AgNPs nanofiber plus SB431542.

deposition during granulation tissue formation and matrix remodeling. The blue-green staining intensity corresponds to the relative quantity of deposited total collagen fiber, which reflects the processes of synthesis, degradation, and remodeling (Figure S2). The results indicated that among the three groups, the PVA/COS-AgNPs nanofiber group had the greatest collagen synthesis. The rate and quantity of collagen formation were the slowest and lowest in the nanofiber plus SB431542 group.

To quantitatively determine the total collagen content in the skin samples, we determined the Hyp content of the wounded skin in each group at different time points.[27] The results indicated that the Hyp contents of all groups increased over time, but the content of the PVA/COS-AgNPs nanofiber group significantly exceeded that of the other groups (Figure 4A), particularly during the early stages of the healing process, whereas the nanofiber plus SB431542 treatment group showed the lowest Hyp content among the three groups during the first 9 days.

The major components of skin collagen are collagen I and collagen III, and many studies show that collagen I and III are closely related to the TGFβ1/Smad signaling pathway.[16,22,28] To investigate collagen fiber production, immunofluorescent staining was used to stain collagen I (green) and collagen III (red) at 3, 7, and 18 days after grafting (Figure 4B–D), and nuclei were counterstained in blue. A confocal laser scanning microscope was used to observe the samples. As shown in Figure S3, collagen I and III deposition increased over time in the three experimental groups, it was increased quickly in the PVA/COS-AgNPs nanofiber group, and plentiful collagen I

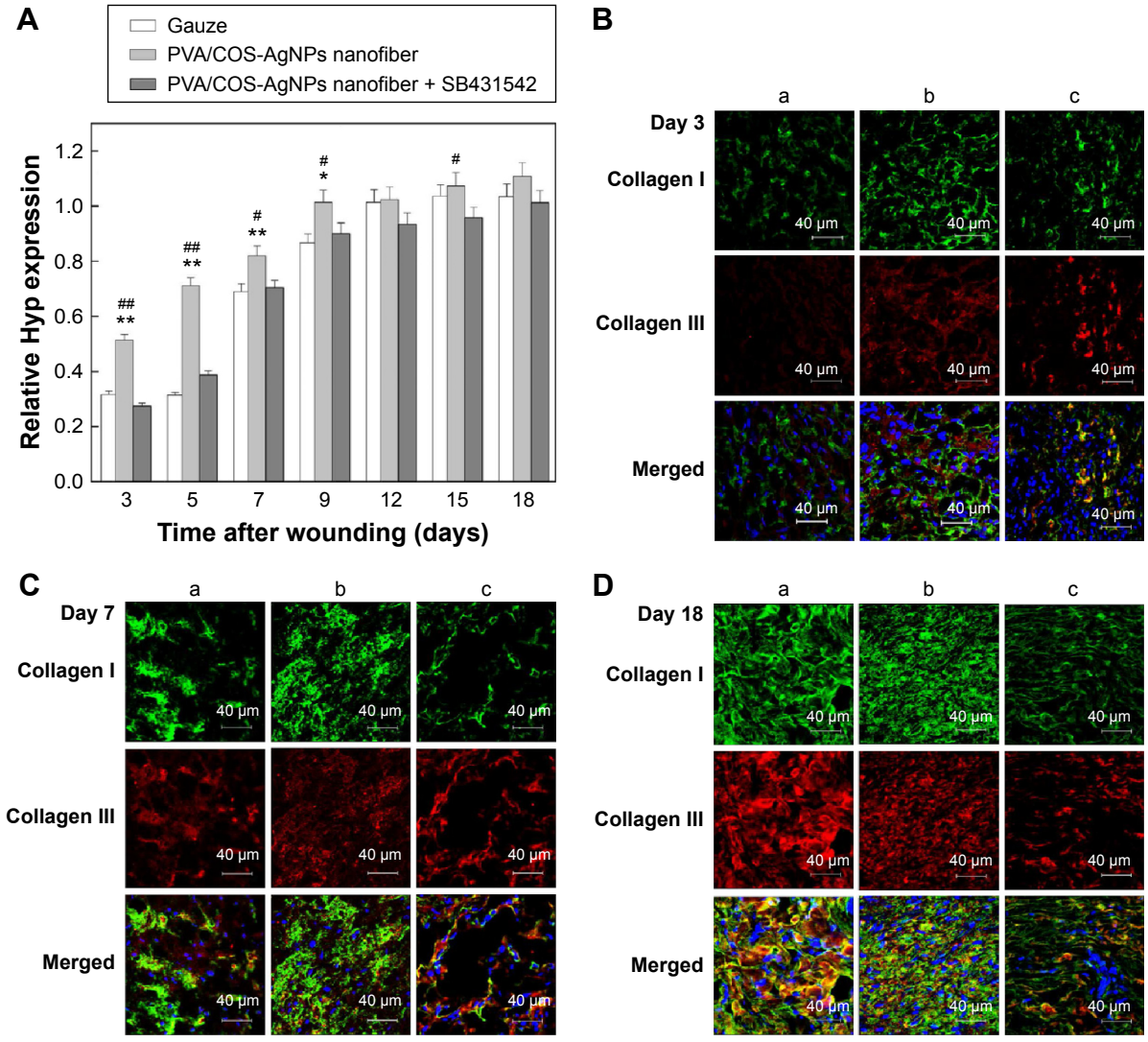

Figure 4 Determination of collagen content in the skin samples.
Notes: (**A**) Hyp content increases in all groups over time, especially in the PVA/COS-AgNPs nanofiber group. (**B**–**D**) Immunofluorescent staining of collagen I (green) and collagen III (red) at 3, 7, and 18 days postgrafting with (a) gauze, (b) PVA/COS-AgNPs nanofiber, (c) PVA/COS-AgNPs nanofiber plus SB431542.
Abbreviations: Hyp, hydroxyproline; PVA, poly(vinyl alcohol); COS, chitosan oligosaccharide; AgNPs, silver nanoparticles.

and III deposition was observed in this group at day 18. Compared with the other two groups, the PVA/COS-AgNPs nanofiber plus SB431542 group had the fewest collagenous fibers at day 18 and the slowest pace of collagen growth.

PVA/COS-AgNPs nanofiber treatment regulates the expression of the TGFβ1/Smad pathway at the gene level

To further investigate the role of the TGFβ1/Smad signaling pathway in PVA/COS-AgNPs nanofiber-induced wound healing, the effects of the PVA/COS-AgNPs nanofiber treatment on wounded skin and the mRNA expression of genes associated with the TGFβ1/Smad signaling pathway were assessed by qRT-PCR. The results showed that the TGFβ1 gene expression was significantly upregulated in the PVA/COS-AgNPs nanofiber group compared with the other groups (Figure 5A). A high level of TGFβ1 expression was observed during the early stage of the wound healing process, particularly at 5 days after surgery. Over time, the TGFβ1 expression decreased slowly, but its expression level in the PVA/COS-AgNPs nanofiber group remained higher than that in the other two groups. The mRNA expression levels of TGFβRI, TGFβRII, collagen I, collagen III, and fibronectin (Figure 5B, C, G–I) exhibited similar results to TGFβ1. Interestingly, Smad2 and Smad3 mRNA expression were upregulated in all three groups; however, no significant differences in this expression were observed between the three groups (Figure 5D and E). In contrast to other genes, Smad7, the inhibitory Smad was upregulated in the three groups over time, and the PVA/COS-AgNPs nanofiber plus SB431542 group showed the greatest upregulation of Smad7 (Figure 5F). Neovascularization is an important process in wound healing,[29] so we also examined the expression of VEGF (Figure S4), a potent and specific angiogenic factor, to investigate the effect on angiogenesis with the PVA/COS-AgNPs nanofiber treatment. The results showed that the highest VEGF expression was observed in the PVA/COS-AgNPs nanofiber group at days 7 and 9, but the difference was not significant among the three groups at the other time points.

PVA/COS-AgNPs nanofiber treatment upregulates proteins associated with the TGFβ1/Smad signaling pathway

Given that gene expression does not usually represent the protein expression level, we next investigated the effects of the PVA/COS-AgNPs nanofiber treatment on the expression of key proteins of the TGFβ1/Smad pathway by performing WB analyses. Our results showed that the TGFβ1 protein expression significantly increased in the PVA/COS-AgNPs nanofiber group during the early stage of the healing process, and over time, the TGFβ1 protein expression decreased. This situation may be associated with the degree of the wound healing (Figure 6). Although the protein expression levels of "total" Smad2 and Smad3 were not significantly different among the three groups, the protein levels of the active forms, phosphorylated Smad2 and 3, were similar to the TGFβ1 protein expression. By contrast, the collagen I and collagen III expression increased over time, and the highest expression was observed in the PVA/COS-AgNPs nanofiber group. In contrast, the nanofiber plus SB431542 group demonstrated the lowest collagen I and collagen III protein expression levels of the three groups during each stage of wound healing. We also evaluated the expression of the active form, phospho-Smad1/5/8. However, the results showed that there was no significant difference in the phospho-Smad1/5/8 expression level between the three groups (data not shown).

Discussion

Wounds occupy a remarkable place in everyday pathology and remain a challenging clinical problem, with many unpredictable complications that frequently result in morbidity and mortality.[30] Wound healing is an extremely complicated process with many influencing factors. Therefore, the investigation of an ideal wound dressing that can achieve rapid healing with minimal inconvenience to patients has been of interest to researchers for a long time.[31] In our previous study, a PVA/COS-AgNPs nanofiber was prepared and applied as a novel wound dressing that had broad-spectrum antibacterial activity and permeability, as well as high porosity. Meanwhile, because of their antibacterial, hemostatic, and anti-inflammatory actions and the ability to stimulate the directional distribution of collagen, the combined action of nanoscale fiber and COS-Ag can accelerate the healing rate of a skin wound, particularly during the early stage of the healing process.[11] Our previous study revealed that the PVA/COS-AgNPs nanofiber has enormous potential for use as a wound dressing; however, the mechanisms by which this treatment promotes wound healing remained unknown. Considering the key role of the TGFβ1/Smad signaling pathway in wound healing, in this study, we used Sprague–Dawley rats to generate a skin wound model and investigated whether the molecular mechanisms by which the PVA/COS-AgNPs nanofiber promotes healing involve this signaling pathway.

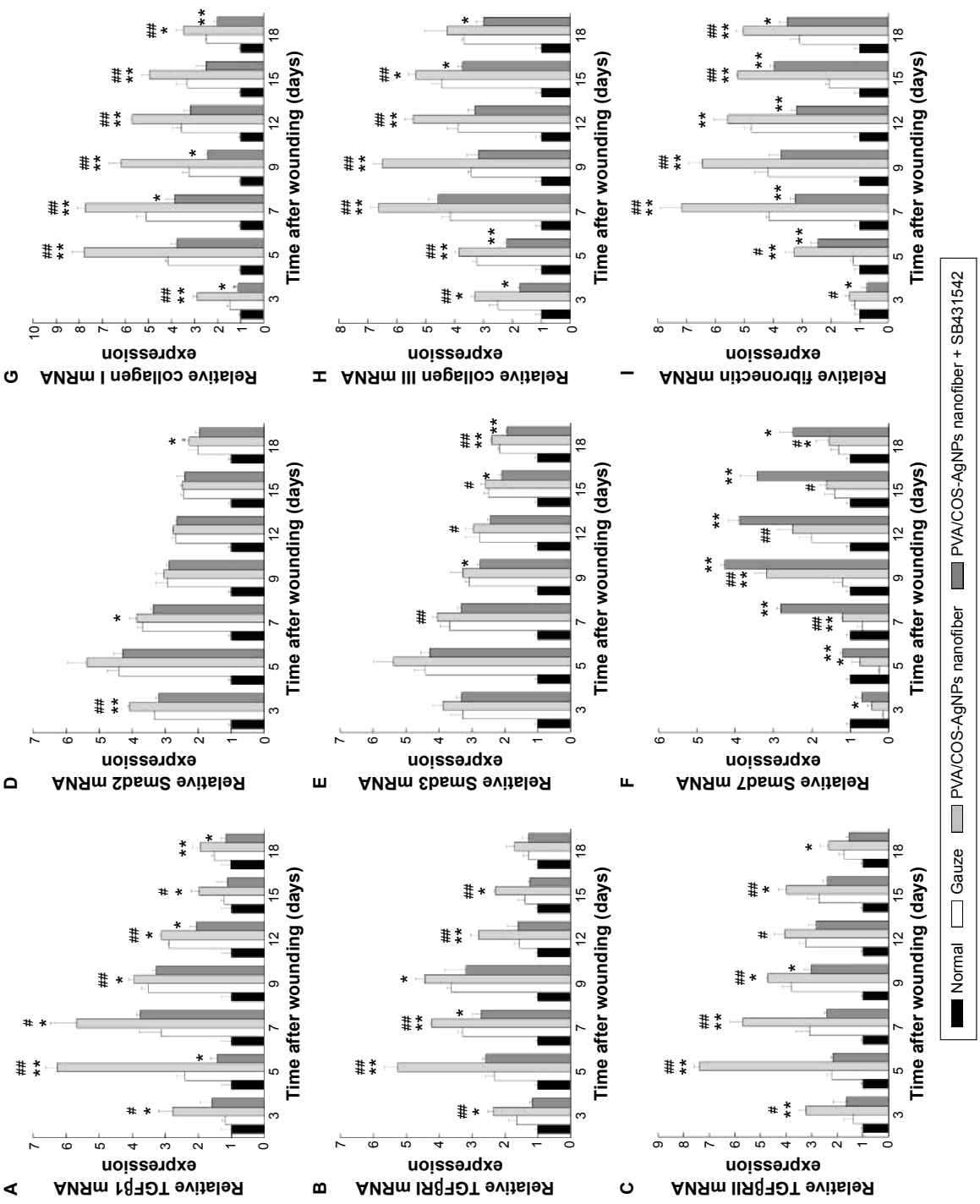

Figure 5 Expression of TGFβ1/Smad pathway at the gene level.

Notes: **(A)** Significant upregulation of TGFβ1 gene expression in PVA/COS-AgNPs nanofiber group. **(B, C, G–I)** mRNA expression levels of TGFβRI, TGFβRII, collagen I, and collagen III showing similar results as TGFβ1. **(D, E)** Smad2 and Smad3 expression was upregulated in all three groups, with no statistically significant difference between the groups. **(F)** PVA/COS-AgNPs nanofiber plus SB431542 showed greatest upregulation of inhibitory Smad, Smad7. Values are mean ± standard deviation. $^{*}P<0.05$ and $^{**}P<0.01$ vs gauze group, $^{\#}P<0.05$ and $^{\#\#}P<0.01$ vs PVA/COS-AgNPs nanofiber plus SB431542 group.

Abbreviations: TGFβ1, transforming growth factor-β1; PVA, poly(vinyl alcohol); COS, chitosan oligosaccharide; AgNPs, silver nanoparticles.

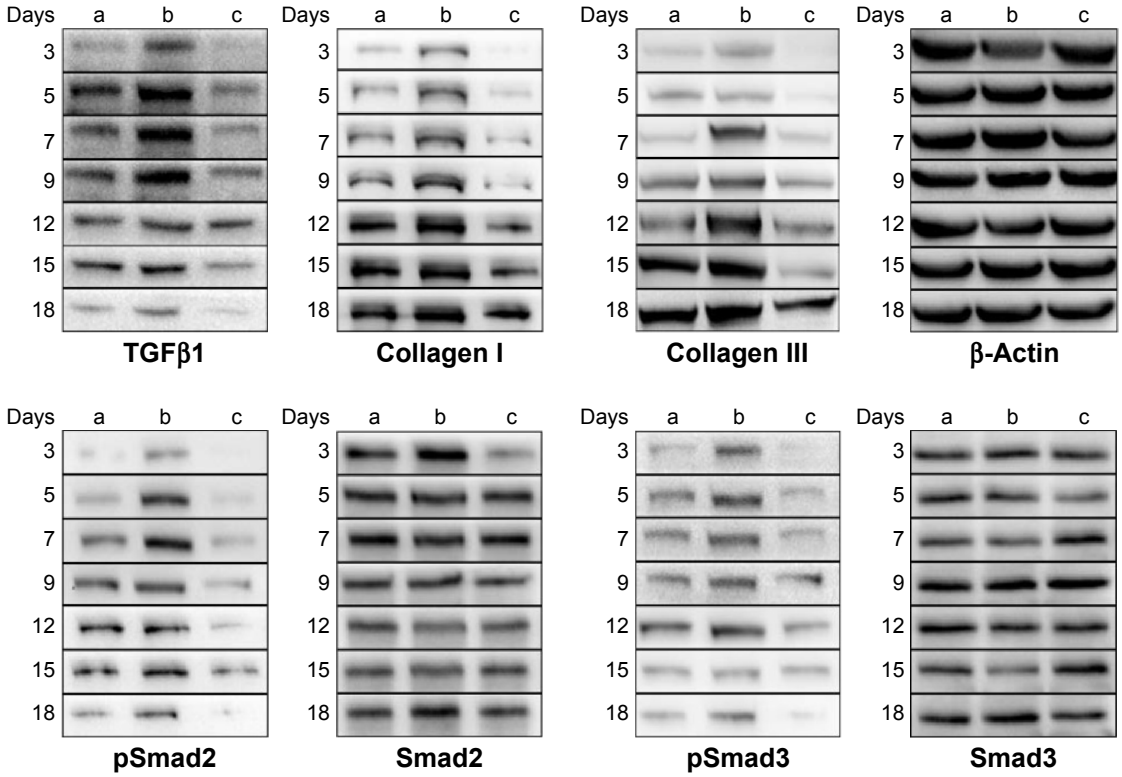

Figure 6 Western blot results of protein expression in the (a) gauze, (b) PVA/COS-AgNPs nanofiber, (c) PVA/COS-AgNPs nanofiber plus SB431542 group at days 3, 5, 7, 9, 12, 15, and 18 after surgery.

Notes: TGFβ1 expression was significantly increased in (b) during the initial stage of the healing process and decreased over time. The active forms, phosphorylated Smad2 and 3, were similar to the TGFβ1 protein expression while the "total" Smad2 and Smad3 were not significantly different among the three groups. Collagen I and collagen III expression increased over time, and the highest expression was observed in (b). In contrast, (c) demonstrated the lowest collagen I and collagen III protein expression levels of the three groups during each stage of wound healing. β-actin served as the internal control.

Abbreviations: TGFβ1, transforming growth factor-β1; PVA, poly(vinyl alcohol); COS, chitosan oligosaccharide; AgNPs, silver nanoparticles.

In this study, our morphological and histological results showed that the PVA/COS-AgNPs nanofiber exerted a potent effect on wound closure and remodeling. The nanofiber plus SB431542 group presented festering wounds during the early stage, and wound remodeling was the slowest in this group throughout the entire healing period. In addition, the healing effect promoted by the PVA/COS-AgNPs nanofiber was further confirmed by HE-stained sections. SB431542 is a specific inhibitor of TGF-β Type I receptor kinase;[32] it specifically binds to the ATP-binding domains of the TGF-β Type I receptor, thus inhibiting Smad2 and Smad3 activation and TGFβ-induced signal transduction, transcription, gene expression, and growth suppression.[33] The aforementioned results show that the PVA/COS-AgNPs nanofiber can promote wound healing, but when SB431542 was combined with the PVA/COS-AgNPs nanofiber, the wound healing process was delayed. These findings were consistent with other findings related to the effect of SB431542[34,35] and with our previous study.[11]

The ECM is an important player in the wound healing process. The ECM not only provides architectural support to the skin but also plays a major role in cell regulation.[36] The ECM is composed primarily of collagen proteins, and inhibition of the TGFβ1/Smad signaling pathway may suppress wound repair by inhibiting collagen production at the early stage of the healing process.[37] Collagen I and collagen III are the two most ubiquitous collagens in the skin,[38] and as ECM-encoding genes, they are direct Smad targets, representing the lynchpins of the Smad pathway in the simultaneous activation of collagen genes by TGFβ1.[39] On the basis of our Masson's trichrome staining, Hyp content, and immunofluorescent staining results, we observed that the PVA/COS-AgNPs nanofiber can stimulate the generation of collagen, whereas the inhibition of the TGFβ1/Smad signaling pathway largely prevented the PVA/COS-AgNPs nanofiber-associated effect on collagen generation at the early stage of the healing process, particularly the effects on collagen I and collagen III. These results further imply that the healing effect promoted by the PVA/COS-AgNPs nanofiber is related to the activation of the TGFβ1/Smad signaling pathway.

Wound healing is regulated by various growth factors and cytokines, and the TGFβ1/Smad signaling pathway is closely related to wound healing.[40–42] When this pathway

is activated, receptor-regulated Smads, such as Smad2 and Smad3, are phosphorylated by TGFβ1 and activin Type I receptors and then complexed with a common-partner Smad called Smad4, which transmits messages to the nucleus and induces the transcription of target genes. The inhibitory Smad, Smad7, plays a role in inhibiting the effect of activated TGFβ receptors, preventing the phosphorylation of Smad2 and Smad3 and downregulating TGFβ1 signaling.[43,44] Thus, the inhibition of Smad7 is thought to increase the rate of wound repair.[45] Our results indicated that PVA/COS-AgNPs nanofiber treatment resulted in significantly increased TGFβ1, TGFβRI, TGFβRII, collagen I, collagen III, and fibronectin mRNA expression during the early stage of wound healing. Conversely, SB431542-induced inhibition of the TGFβ1/Smad signaling pathway downregulated the expression of these genes. The Smad7 level of the three groups was upregulated over time, whereas in the PVA/COS-AgNPs nanofiber plus SB431542 group, this level was more upregulated. Interestingly, the levels of Smad2 and Smad3, the only downstream mediators of TGFβRI that are central to most actions of the TGFβ family regarding ECM gene expression,[46] were upregulated in all three groups; however, no significant differences in expression were observed between these groups. These results represent an imbalance in the agonistic Smad proteins. The peak amount of VEGF mRNA occurred latest in the PVA/COS-AgNPs nanofiber plus SB431542 group compared with the other two groups. We inferred that the possible cause of these results was connected to the PVA/COS-AgNPs nanofiber plus SB431542 group having the slowest healing process and the latest growth time of granulation tissue compared with those of the other groups. Although the mRNA levels of target genes may not necessarily cause changes in the signal transduction of a signaling pathway or in the expression of the corresponding proteins, the results also support the observation that the PVA/COS-AgNPs nanofiber can activate the TGFβ1/Smad signaling pathway.

In the TGFβ1/Smad signaling pathway, signals can only be transduced when Smad2 and Smad3 are phosphorylated to their active forms.[47,48] In our encouraging WB results, the protein levels of the active forms phospho-Smad2 and phospho-Smad3 significantly increased in the PVA/COS-AgNPs nanofiber group during the early stage of the healing progress. The protein expression levels of TGFβ1, collagen I, and collagen III exhibited trends that were consistent with their mRNA expression levels in the PVA/COS-AgNPs nanofiber group. The usage of SB431542 can counteract the PVA/COS-AgNPs nanofiber-induced upregulation of proteins involved in the TGFβ1/Smad signaling pathway. These results clearly demonstrated the activation of the TGFβ1/Smad signaling pathway by PVA/COS-AgNPs nanofiber. Furthermore, although TGFβ1 can activate the Smad1/5/8 pathway by binding the ALK1 receptor, our PVA/COS-AgNPs nanofiber did not seem to affect the activation of Smad1/5/8; instead, it mainly promotes wound healing via the TGFβ1-Smad2/3 pathway.

In conclusion, our results demonstrated that the PVA/COS-AgNPs nanofiber promotes wound healing by activating the TGFβ1/Smad signaling pathway. Inhibition of this pathway largely prevented the PVA/COS-AgNPs nanofiber-associated salutary effects on the early stage of wound healing, thus supporting our conclusion. The activation of a signaling pathway is the summation of the joint effects exerted by many factors, and Ag, COS, and PVA along with the nanotopography all contributed to these described combined actions. This study contributes to a better understanding of the mechanism underlying the accelerated healing effect of the PVA/COS-AgNPs nanofiber.

Acknowledgment

We gratefully acknowledge the financial support received from the Chongqing Programs for Application and Development (cstc2014yykfA110022).

Disclosure

The authors report no conflicts of interest in this work.

References

1. Wu Z, Tang Y, Fang H, et al. Decellularized scaffolds containing hyaluronic acid and EGF for promoting the recovery of skin wounds. *J Mater Sci*. 2015;26:1–10.
2. Delavary BM, van der Veer WM, van Egmond M, et al. Macrophages in skin injury and repair. *Immunobiology*. 2011;216:753–762.
3. Pereira RF, Barrias CC, Granja PL, et al. Advanced biofabrication strategies for skin regeneration and repair. *Nanomedicine*. 2013;8:603–621.
4. Sandeep K, Maiti SK, Naveen K, et al. Effect of medical grade chitosan powder in full thickness skin wound healing in rat model. *J Anim Vet Adv*. 2014;2:270–276.
5. Rieger KA, Birch NP, Schiffman JD. Designing electrospun nanofiber mats to promote wound healing – a review. *J Mater Chem B*. 2013;1:4531–4541.
6. Zahedi P, Rezaeian I, Ranaei-Siadat SO, et al. A review on wound dressings with an emphasis on electrospun nanofibrous polymeric bandages. *Polym Adv Technol*. 2010;21:77–95.
7. Muzzarelli RAA, Muzzarelli C. Chitosan chemistry: relevance to the biomedical sciences. *Adv Polym Sci*. 2005;151–209.
8. Liu X, Xia W, Jiang Q, et al. Effect of kojic acid-grafted-chitosan oligosaccharides as a novel antibacterial agent on cell membrane of gram-positive and gram-negative bacteria. *J Biosci Bioeng*. 2015;120(3):335–339.
9. Xia W, Liu P, Zhang J, et al. Biological activities of chitosan and chitooligosaccharides. *Food Hydrocolloids*. 2011;25:170–179.
10. Liu X, Xia W, Jiang Q, et al. Synthesis, characterization, and antimicrobial activity of kojic acid grafted chitosan oligosaccharide. *J Agric Food Chem*. 2013;62:297–303.

11. Li C, Fu R, Yu C, et al. Silver nanoparticle/chitosan oligosaccharide/poly(vinyl alcohol) nanofibers as wound dressings: a preclinical study. *Int J Nanomed*. 2013;8:4131.
12. Li L, Zhu Z, Xiao W. Multi-walled carbon nanotubes promote cementoblast differentiation and mineralization through the TGF-β/Smad signaling pathway. *Int J Mol Sci*. 2015;16:3188–3201.
13. Cichon MA, Radisky DC. Extracellular matrix as a contextual determinant of transforming growth factor-b signaling in epithelial-mesenchymal transition and in cancer. *Cell Adhes Migrat*. 2014;8(6):588–594.
14. Leask A. New insights into the basis of the activated fibroblast phenotype in scleroderma. *Adv Skin Wound Care*. 2011;2:210–216.
15. Tang B, Zhu B, Liang Y, et al. Asiaticoside suppresses collagen expression and TGF-β/Smad signaling through inducing Smad7 and inhibiting TGF-βRI and TGF-βRII in keloid fibroblasts. *Arch Dermatol Res*. 2011;303:563–572.
16. Ganeshkumar M, Ponrasu T, Krithika R, et al. Topical application of Acalypha indica accelerates rat cutaneous wound healing by up-regulating the expression of Type I and III collagen. *J Ethnopharmacol*. 2012;142:14–22.
17. Verrecchia F, Mauviel A. Control of connective tissue gene expression by TGFβ: role of Smad proteins in fibrosis. *Curr Rheumatol Rep*. 2002;4:143–149.
18. Hu PP-C, Datto MB, Wang X-F. Molecular mechanisms of transforming growth factor-β signaling. *Endocr Rev*. 1998;19:349–363.
19. Itoh S, Itoh F, Goumans MJ, et al. Signaling of transforming growth factor-β family members through Smad proteins. *Eur J Biochem*. 2000;267:6954–6967.
20. Diegelmann RF, Evans MC. Wound healing: an overview of acute, fibrotic and delayed healing. *Front Biosci*. 2004;9:283–289.
21. Bhawal UK, Lee H-J, Uchida R, et al. The pro-healing effect of protamine-hydrolysate peptides on skin wounds involves TGF-β/Smad signaling. *J Hard Tissue Biol*. 2015;24:91–98.
22. Shi H-X, Lin C, Lin B-B, et al. The anti-scar effects of basic fibroblast growth factor on the wound repair in vitro and in vivo. *PloS One*. 2013;8:e59966.
23. Inman GJ, Nicolás FJ, Callahan JF, et al. SB-431542 is a potent and specific inhibitor of transforming growth factor-β superfamily type I activin receptor-like kinase (ALK) receptors ALK4, ALK5, and ALK7. *Mol Pharmacol*. 2002;62:65–74.
24. Shivananda BN, Vincent R, Sandeep M, et al. Wound healing activity of the fruit skin of Punica granatum. *J Med Food*. 2013;16:857–861.
25. Oxlund H, Christensen H, Seyer-Hansen M, et al. Collagen deposition and mechanical strength of colon anastomoses and skin incisional wounds of rats. *J Surg Res*. 1996;66:25–30.
26. Dorsett-Martin WA. Rat models of skin wound healing: a review. *Wound Repair Regen*. 2004;12:591–599.
27. Pang Y, Wang D, Hu X, et al. Effect of volatile oil from Blumea Balsamifera (L.) DC. leaves on wound healing in mice. *J Tradit Chin Med*. 2014;34:716–724.
28. Rosensteel SM, Wilson RP, White SL, et al. COL1A1 oligodeoxynucleotides decoy: biochemical and morphologic effects in an acute wound repair model. *Exp Mol Pathol*. 2010;89:307–313.
29. Ud-Din S, Sebastian A, Giddings P, et al. Angiogenesis is induced and wound size is reduced by electrical stimulation in an acute wound healing model in human skin. *PloS One*. 2015;10:1–22.
30. Velnar T, Bailey T, Smrkolj V. The wound healing process: an overview of the cellular and molecular mechanisms. *J Int Med Res*. 2009;37:1528–1542.
31. Boateng JS, Matthews KH, Stevens HN, et al. Wound healing dressings and drug delivery systems: a review. *J Pharm Sci*. 2008;97:2892–2923.
32. Laping N, Grygielko E, Mathur A, et al. Inhibition of transforming growth factor (TGF)-β1–induced extracellular matrix with a novel inhibitor of the TGF-β type I receptor kinase activity: SB-431542. *Mol Pharmacol*. 2002;62:58–64.
33. Halder SK, Beauchamp RD, Datta PK. A specific inhibitor of TGF-β receptor kinase, SB-431542, as a potent antitumor agent for human cancers. *Neoplasia*. 2005;7:509–521.
34. Sakai H, Matsuura K, Tanaka Y, et al. Signaling mechanism underlying the promotion of keratinocyte migration by angiotensin II. *Mol Pharmacol*. 2015;87:277–285.
35. Sugiyama K, Ishii G, Ochiai A, et al. Improvement of the breaking strength of wound by combined treatment with recombinant human G-CSF, recombinant human M-CSF, and a TGF-β1 receptor kinase inhibitor in rat skin. *Cancer Sci*. 2008;99:1021–1028.
36. Maquart F, Monboisse J. Extracellular matrix and wound healing. *Pathol Biol*. 2014;62:91–95.
37. Yamaoka H, Sumiyoshi H, Higashi K, et al. A novel small compound accelerates dermal wound healing by modifying infiltration, proliferation and migration of distinct cellular components in mice. *J Dermatol Sci*. 2014;74:204–213.
38. Fathke C, Wilson L, Hutter J, et al. Contribution of bone marrow–derived cells to skin: collagen deposition and wound repair. *Stem Cells*. 2004:22:812–822.
39. Verrecchia F, Chu M-L, Mauviel A. Identification of novel TGF-β/Smad gene targets in dermal fibroblasts using a combined cDNA microarray/promoter transactivation approach. *J Biol Chem*. 2001;276:17058–17062.
40. Schiller M, Javelaud D, Mauviel A. TGF-β-induced SMAD signaling and gene regulation: consequences for extracellular matrix remodeling and wound healing. *J Dermatol Sci*. 2004;35:83–92.
41. Martin P. Wound healing – aiming for perfect skin regeneration. *Science*. 1997;276:75–81.
42. Beldon P. Basic science of wound healing. *Surgery (Oxford)*. 2010;28:409–412.
43. Heldin C-H, Miyazono K, Ten Dijke P. TGF-β signalling from cell membrane to nucleus through SMAD proteins. *Nature*. 1997;390:465–471.
44. Xu L, Zheng N, He Q, et al. Puerarin, isolated from Pueraria lobata (Willd.), protects against hepatotoxicity via specific inhibition of the TGF-β1/Smad signaling pathway, thereby leading to anti-fibrotic effect. *Phytomedicine*. 2013;20:1172–1179.
45. Reynolds LE, Conti FJ, Silva R, et al. α3β1 integrin–controlled Smad7 regulates reepithelialization during wound healing in mice. *J Clin Invest*. 2008;118:965.
46. Takagawa S, Lakos G, Mori Y, et al. Sustained activation of fibroblast transforming growth factor-β/Smad signaling in a murine model of scleroderma. *J Invest Ddermatol*. 2003;121:41–50.
47. Miyazono K, Ten Dijke P, Heldin C-H. TGF-β signaling by Smad proteins. *Adv Immunol*. 2000;75:115–157.
48. Lee K-B, Jeon J-H, Choi I, et al. Clusterin, a novel modulator of TGF-β signaling, is involved in Smad2/3 stability. *Biochem Biophy Res Commun*. 2008;366:905–909.

Supplementary materials

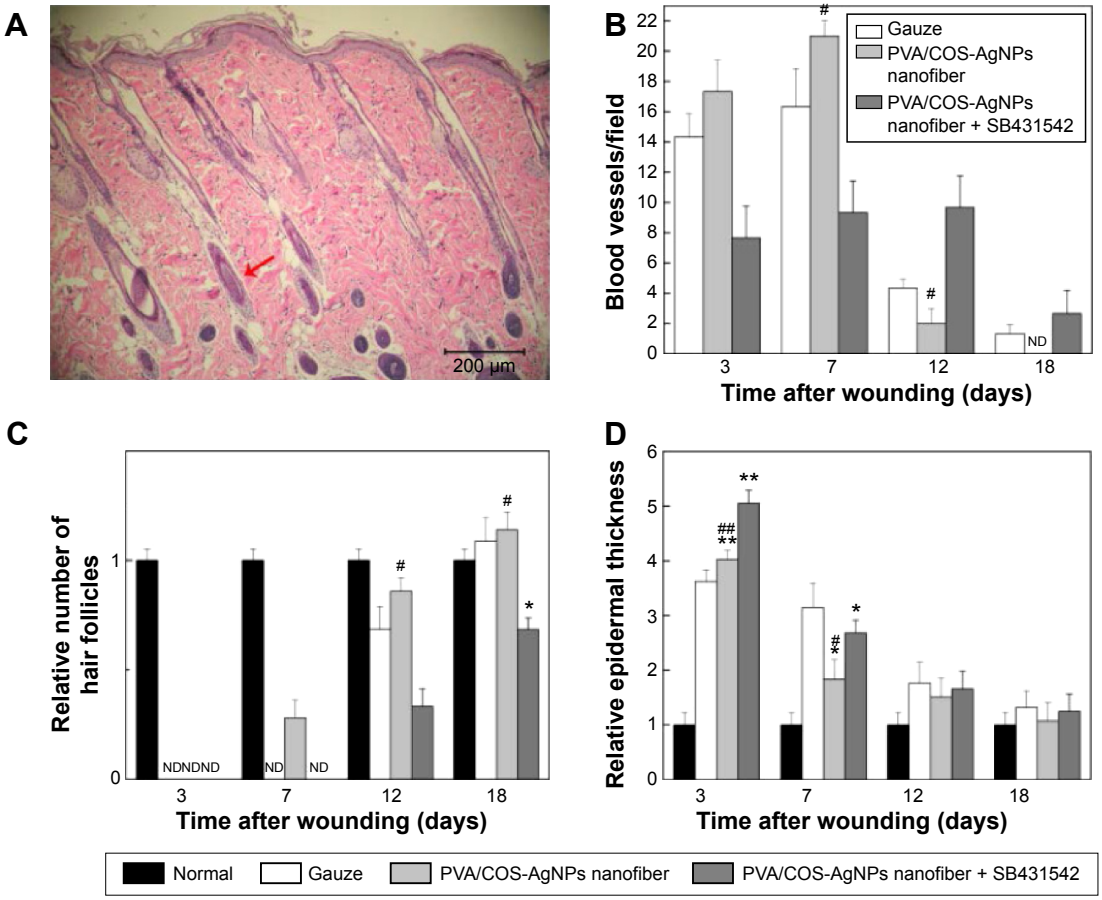

Figure S1 The histology of normal skin and the histologic associated comparison of the three groups.

Notes: (A) The HE staining of normal skin. The arrows colored with red indicates hair follicles. (**B**) The number of blood vessels of the same multiples' field (×100) in normal, gauze, PVA/COS-AgNPs nanofiber, PVA/COS-AgNPs nanofiber plus SB431542 at 3, 7, 12, 18 days post-wounding. (**C**) The relative number of hair follicles in normal, gauze, PVA/COS-AgNPs nanofiber, PVA/COS-AgNPs nanofiber plus SB431542 at 3, 7, 12, 18 days post-wounding. (**D**) The relative thickness of the epidermis in normal, gauze, PVA/COS-AgNPs nanofiber, PVA/COS-AgNPs nanofiber plus SB431542 at 3, 7, 12, 18 days post-wounding. Values are mean ± standard deviation. $^{*}P<0.05$ and $^{**}P<0.01$ vs normal group, $^{\#}P<0.05$ and $^{\#\#}P<0.01$ vs PVA/COS-AgNPs nanofiber plus SB431542 group.

Abbreviations: PVA, poly(vinyl alcohol); COS, chitosan oligosaccharide; AgNPs, silver nanoparticles; ND, no data; HE, hematoxylin–eosin.

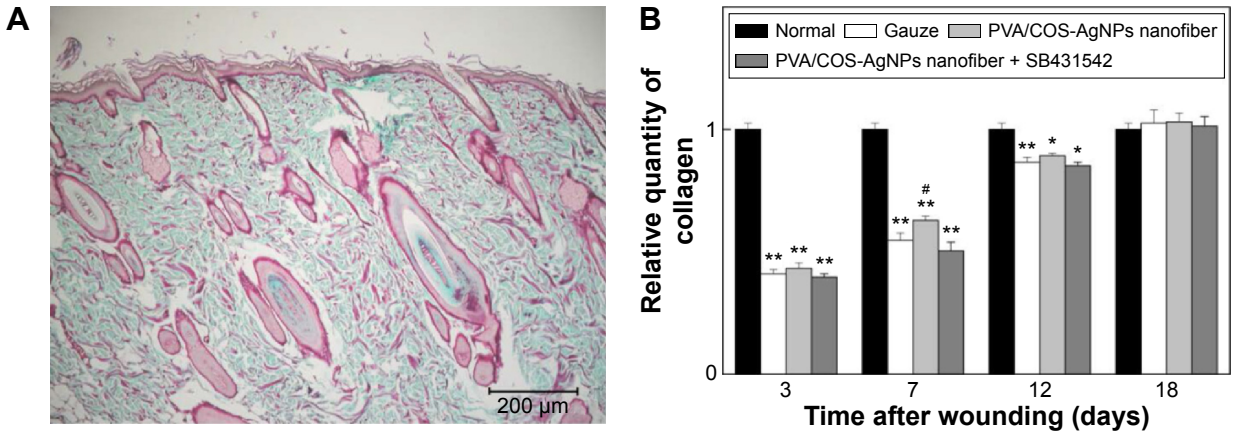

Figure S2 Collagen fiber regeneration in rat skin.

Notes: (**A**) Masson-trichrome staining of normal skin. Blue-green staining intensity corresponds to relative quantity of deposited collagen fiber. (**B**) The relative quantity of collagen in normal, gauze, PVA/COS-AgNPs nanofiber, PVA/COS-AgNPs nanofiber plus SB431542 at 3, 7, 12, 18 days post-wounding. PVA/COS-AgNPs nanofiber group showed the greatest collagen synthesis. Values are mean ± standard deviation. $^{*}P<0.05$ and $^{**}P<0.01$ vs normal group, $^{\#}P<0.05$ and $^{\#\#}P<0.01$ vs PVA/COS-AgNPs nanofiber plus SB431542 group.

Abbreviations: PVA, poly(vinyl alcohol); COS, chitosan oligosaccharide; AgNPs, silver nanoparticles.

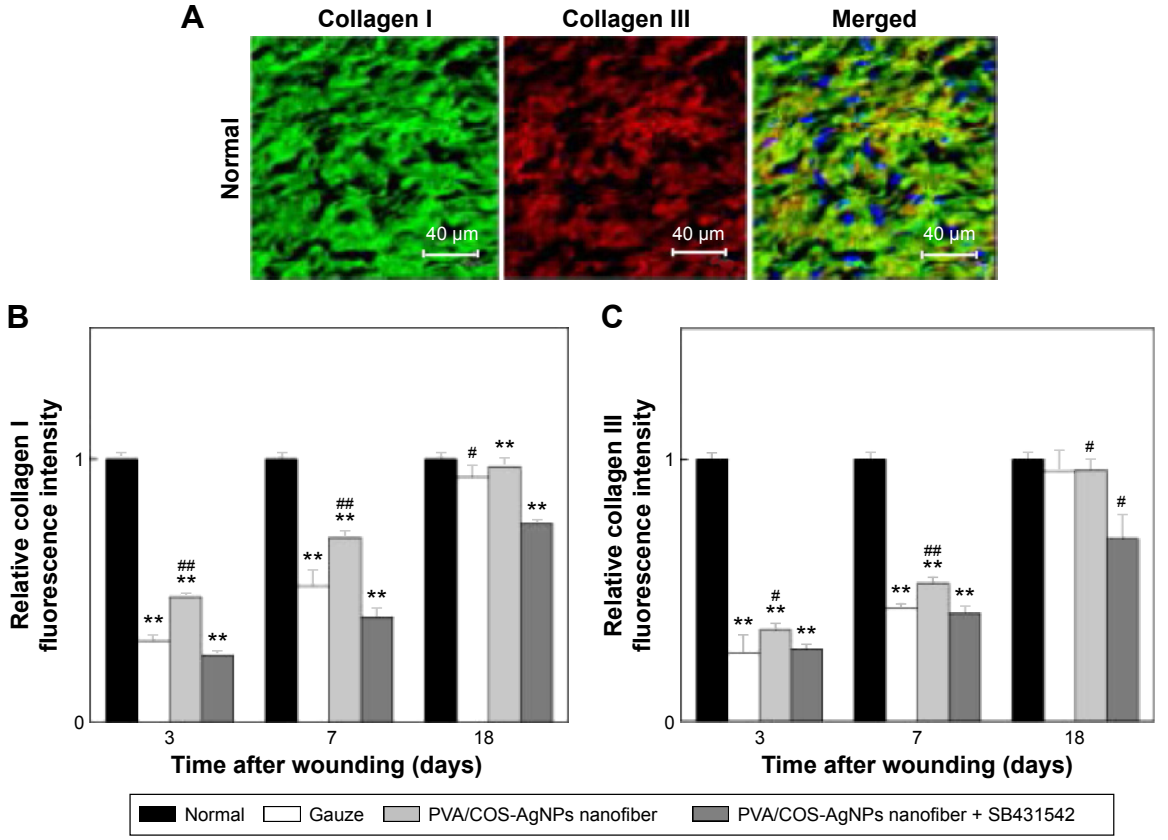

Figure S3 Increase in deposition of collagen I and collagen III over time in the three groups.
Notes: (**A**) Immunofluorescent staining of collagen I and collagen III of normal skin (×800). (**B**) The relative collagen I fluorescence intensity in normal, gauze, PVA/COS-AgNPs nanofiber, PVA/COS-AgNPs nanofiber plus SB431542 at 3, 7, 12, 18 days post-wounding. (**C**) The relative collagen III fluorescence intensity in normal, gauze, PVA/COS-AgNPs nanofiber, PVA/COS-AgNPs nanofiber plus SB431542 at 3, 7, 12, 18 days post-wounding. Increased deposition of collagen I and III were observed in the PVA/COS-AgNPs nanofiber group at day 18. Values are mean ± standard deviation. $^{*}P<0.05$ and $^{**}P<0.01$ vs normal group, $^{\#}P<0.05$ and $^{\#\#}P<0.01$ vs PVA/COS-AgNPs nanofiber plus SB431542 group.
Abbreviations: PVA, poly(vinyl alcohol); COS, chitosan oligosaccharide; AgNPs, silver nanoparticles.

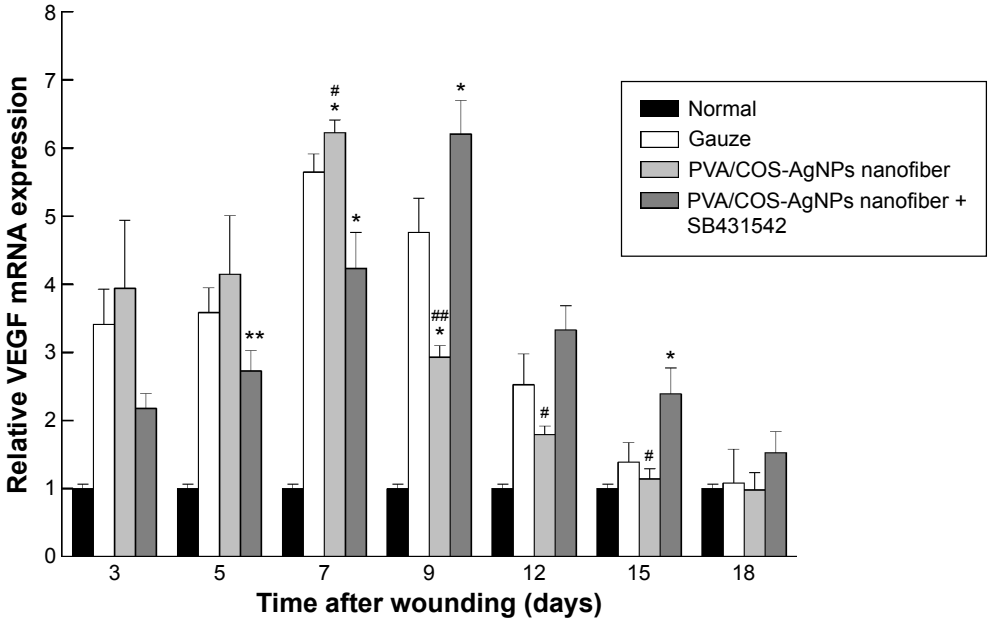

Figure S4 VEGF expression to study the effect of angiogenesis on wound healing.
Notes: Highest VEGF expression was observed in PVA/COS-AgNPs nanofiber group. Values are mean ± standard deviation. $^{*}P<0.05$ and $^{**}P<0.01$ vs gauze group, $^{\#}P<0.05$ and $^{\#\#}P<0.01$ vs PVA/COS-AgNPs nanofiber plus SB431542 group.
Abbreviations: VEGF, vascular endothelial growth factor; PVA, poly(vinyl alcohol); COS, chitosan oligosaccharide; AgNPs, silver nanoparticles.